The influence of calcium and copper on the structure of alloys in the cross-linked Al –Mg – Zn – Ca – Cu system

V. V. Doroshenko, *Candidate of Technical Sciences, Senior Researcher of the Department "Materials Science", Associate Professor of the Project Activity Sector*[1], *e-mail: v.doroshenko@mail.ru*
R. R. Saifutyarov, *Candidate of Chemical Sciences, Senior Researcher*[2], *Research Chemical and Analytical Center NRC "Kurchatov Institute" Shared Research Facilities, e-mail:rosya01@gmail.com*
A. A. Aksenov, *Doctor of Technical Sciences, Professor, Chief Researcher of the Department "Physics"*[1], *e-mail:a_aksenov_59@mail.ru*
V. V. Eremeeva, *Lecturer of the Department "Foreign Language"*[1], *e-mail: EremeevaV@bk.ru*

[1]*Moscow Polytechnic University (Moscow Polytech), Moscow, Russia.*
[2]*National Research Centre "Kurchatov Institute", Moscow, Russia.*

This study presents the results of phase composition determination for four alloys in the Al – Mg – Zn – Ca – Cu system. The analysis was performed using both computational (Thermo-Calc) and experimental (DSC, SEM) methods. According to cooling curves based on the Scheil model, the studied alloys exhibit similar liquidus temperatures (613–620 °C) but different solidus temperatures, which decrease with increasing copper content. Conversely, the non-equilibrium solidus temperature increases. These findings align well with DSC results, indicating that solidus temperature shows significant differences only in copper-containing alloys, with higher values by 20–30 °C. The cast microstructure of all alloys is characterized by a degenerate eutectic nature, with an average crystal size up to 4 μm by Feret, and the calculated volume fraction of secondary phases did not exceed 12 vol.%. The aluminum matrix was enriched with magnesium, zinc, and copper, while zinc content remained unchanged with increasing calcium and copper concentrations. As calcium content increased to 1.5%, zinc solubility in the Al_4Ca phase decreased, reaching a minimum at 1.5% Ca and 1% Cu. Copper solubility increased with its content in the alloy; however, after quenching at 440 °C for 3 hours, zinc and copper solubility in the Al_4Ca phase increased. In copper-containing alloys, two additional copper-containing phases were identified after furnace cooling, besides $(Al,Zn,Cu)_4Ca$ and *T* (AlMgZnCu). At 0.5% Cu, the AlCuMg phase was detected, which was absent at 1% Cu; instead, a ternary compound $Al_{27}Ca_3Cu_7$ formed, incorporating up to 6 at.% zinc.

Key words: Aluminum, magnesium, calcium, copper, phases, phase transformations, microstructure.
DOI: 10.17580/nfm.2025.01.07

Introduction

The 5xxx series of wrought alloys (Al – Mg) have found a wide range of applications in marine [1, 2] and land transport [3] due to a good combination of properties such as high strength to weight ratio, good ductility, excellent corrosion resistance and weldability. The enhanced strength of these alloys is attributable to two principal mechanisms: the hardening of the solid solution with magnesium, and strain hardening during the rolling process. Nevertheless, the yield strength remains at a comparatively low level. The addition of zinc to Al – Mg alloys has been shown to result in a substantial enhancement of their mechanical characteristics. The resulting phases, such as $Al_2Mg_3Zn_3$ or $Mg_{32}(Al,Zn)_{49}$ (*T′* phase) and $MgZn_2$ (η′ phase), play a key role in improving the mechanical properties. The addition of zinc allows heat treatment (HT), during which the aluminium solid solution decomposes, releasing hardening dispersoids of the metastable phases *T′* [4–6] and/or η′ [7]. However, elevated zinc concentrations significantly increase the density of the alloy, which removes one of the main advantages of alloys from such alloying systems compared with high-strength 7xxx series alloys and medium-strength 6xxx series alloys.

The addition of calcium, which has a low density and forms a eutectic type diagram with aluminium, appears to be a promising option [8–10]. A number of papers have recently been published on alloys based on the system Al – Zn – Mg – Ca [11–14]. Concurrently, there has been a paucity of attention paid to compositions containing less zinc than magnesium and aimed at obtaining heat-strengthenable alloys. A distinctive feature of joint alloying with calcium and zinc is the fact that zinc has significant solubility in the Al_4Ca phase [8]. Indeed, the mass fraction of zinc may exceed that of calcium. In the case of alloys with Zn : Mg ratios ≤ 1, this can be an obstacle in the development of heat-strengthenable alloys.

It was established that both copper and zinc have the capacity to dissolve within the Al_4Ca phase [8, 15, 16]. To date, there has been no published work considering the

Table 1
Chemical composition of the investigated alloys

Alloy	Marking	Al, wt.%	Main alloying elements, wt.%				Fe, wt.%
			Mg	Zn	Ca	Cu	
Al5.5Mg4Zn1Ca	1Ca0Cu	Bal.	5.57	3.78	0.85	–	0.3
Al5.5Mg4Zn1.5Ca	1.5Ca0Cu	Bal.	5.76	3.7	1.69	–	0.19
Al5Mg4Zn1.5Ca0.5Cu	1.5Ca0.5Cu	Bal.	5.24	3.7	1.63	0.7	0.18
Al5Mg4Zn1.5Ca1Cu	1.5Ca1Cu	Bal.	4.81	3.78	1.57	1.22	0.2

Table 2
Calculated phase composition of the investigated alloys at temperature 25 °C*

Phase	Chemical elements, wt.%						Alloy
	Al	Mg	Zn	Ca	Cu	Fe	
Al_3Fe	Rest	–	–	–	–	40.8	1Ca0Cu
Al_4Ca	Rest	–	–	27.1	–	–	
(Al)	Rest	0.2	<0.01	<0.01	<0.01	<0.01	
T	Rest	30.7	21.5	–	–	–	
Al_3Fe	Rest	–	–	–	–	40.8	1.5Ca0Cu
Al_4Ca	Rest	–	–	27.1	–	–	
(Al)	Rest	0.2	<0.01	<0.01	<0.01	<0.01	
T	Rest	30.9	20.5	–	–	–	
Al_3Fe	Rest	–	–	–	<0.01	40.8	1.5Ca0.5Cu
Al_4Ca	Rest	–	–	27.1	–	–	
(Al)	Rest	0.2	<0.01	<0.01	<0.01	<0.01	
T#1	Rest	29.8	22.0	–	3.71	–	
T#2	Rest	29.3	15.6	–	13.0	–	
Al_3Fe	Rest	–	–	–	<0.01	40.8	1.5Ca1Cu
Al_4Ca	Rest	–	–	27.1	–	–	
(Al)	Rest	0.3	<0.01	<0.01	<0.01	<0.01	
T#1	Rest	28.6	23.8	–	7.7	-	

*The composition of the alloy 1.5Ca1Cu is given at 50 °C due to the complexity involved in delineating phase boundaries at lower temperatures.

Al – Zn – Cu – Ca or Al–Mg – Zn – Cu – Ca systems. Consequently, the manner in which these elements interact with each other remains ambiguous. Additionally, the feasibility of zinc substitution in the Al_4Ca phase in the presence of copper additions remains to be elucidated. Considering the fact that the release of additional zinc concentrations for the formation of strengthening dispersoids is important, it is of interest to study the phase composition of alloys of the Al – Mg – Zn – Ca – Cu system.

Research methods

The objects of the study were four alloys of the Al – Mg – Zn – Ca – Cu system. The actual compositions and marking of the alloys are given in **Table 1**. Subsequent discussion will refer to the alloys according to their marking. The selection of calcium and copper concentrations was informed by extant research. In accordance with the findings of studies [17–19], it can be hypothesised that the presence of calcium content exceeding 3% will precipitate two consequences: the genesis of coarse eutectic crystals of the Al_4Ca phase, which have the potential to exert a deleterious effect on deformation processing, and an augmented dissolution of zinc within the Al_4Ca phase. Consequently, the present study was constrained to lower calcium concentrations. Conversely, the addition of more than 0.5% Cu has been shown to enhance both corrosion resistance [20] and strength [21].

The alloys were obtained from pure components, using primary aluminium grade A8 (GOST 11069–2019), magnesium grade Mg90 (GOST 804–93), zinc grade C0 (GOST 3640–94), calcium of 99% purity (TU 20.13.23-001-45034953–2022) and copper grade M1 (GOST 859–2001). The melting process was conducted within a resistance furnace operated by the GRAFCARBO company (Italy), utilising graphite crucibles. The sequence of melting processes involved the following: initial melting of aluminium, melting of copper (for the production of aluminium alloys), melting of calcium, melting of magnesium and zinc, and casting into a graphite mould at a temperature of 730 °C without preheating of the mould. Consequently, flat ingots with dimensions of 15×30×180 mm were obtained. Subsequent to this, samples were extracted from the ingots for the purpose of determining the chemical compositions of the alloys and for the study of the microstructure. The preparation of samples for microstructural studies was conducted through abrasing machining and polishing using a diamond suspension. Following this, the samples were subjected to etching in a 0.5% HF solution for a period of 20 seconds. The actual compositions were established through calculations of fragments of state diagrams, which were used to establish the boundaries of phase regions, determine the phase composition and critical temperatures of phase transformations. The implementation of this stage of the study was performed in the computer programme Thermo-Calc version TCW5, database TTAl5 [22]. The microstructure and phase composition of the alloys were analysed in both their cast and heat-treated states. The analysis was conducted using a scanning electron microscope (JSM-7100F, Oxford Instruments X-Max 50 detector, accelerating voltage in the microscope column of 10 kV) and a differential scanning calorimeter (ZCT-B). The

thermal treatment was carried out in an SNOL 8.2/1100 electric furnace, with a temperature maintenance accuracy of ±1 °C. Quantitative parameters of the structure were evaluated using software tools: ImageJ and Origin Pro 18.

Results and discussion

Thermodynamic calculations

The investigation revealed the following set of phases to be present in the selected Thermo-Calc database in the solid state. The alloys of the Al – Mg – Zn – Ca – Cu system investigated were found to contain phases of the following composition, as presented in **Table 2**.

The nature of crystallization, especially under conditions other than ideal, is best described by the Scheil non-equilibrium crystallization curves **(Figs. 1, *a–d*)**. These curves demonstrate that all selected alloys initiate crystallization with the formation of aluminium solid solution. Furthermore, the calculation indicates that the crystallization process of all alloys is analogous, with the initial formation of Al_3Fe crystals, followed by Al_4Ca, and

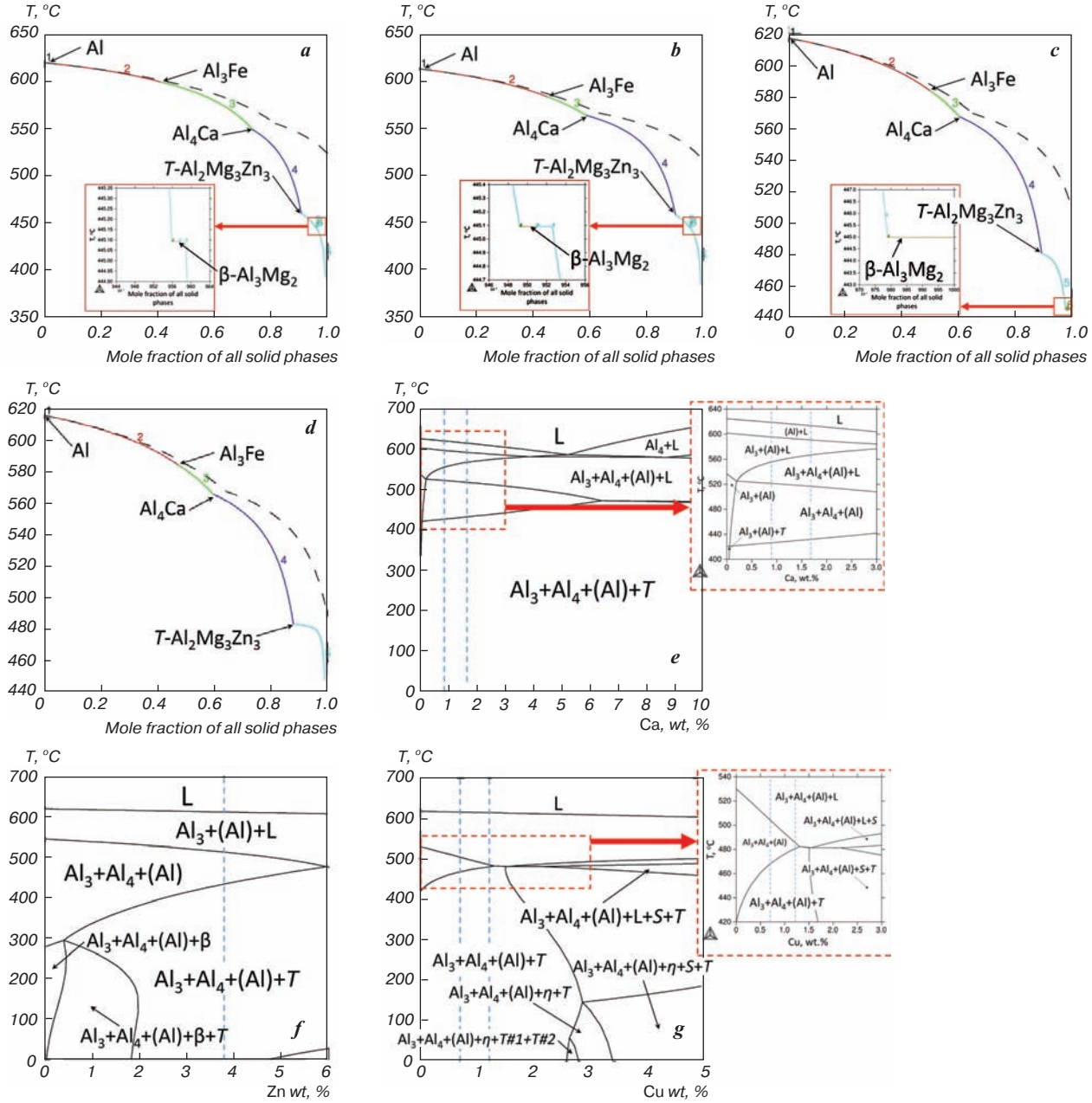

Fig. 1. Aligned Scheil curves of equilibrium and non-equilibrium crystallization (*a–d*) and thermodynamic calculations of Al – Mg – Zn – Ca – Cu phase diagram fragments (*e–g*): *a–d* – combined equilibrium and nonequilibrium crystallization curves for the alloys (*a* – 1Ca0Cu, *b* – 1.5Ca0Cu, *c* – 1.5Ca0.5Cu, *d* – 1. 5Ca1Cu); *e* – polythermal cross section at 5.65% Mg, 3.74% Zn, 0.25% Fe; *f* – polythermal cross section at 5.76% Mg, 1.69% Ca, 0.19% Fe; *g* – polythermal cross section at 5% Mg, 1.6%Ca, 3.74% Zn, 0.19%Fe. The dashed line in plots *a–d* indicates the equilibrium crystallization curve. The vertical lines in figures e-g denote the position of the alloys. In images *e–g*, the abbreviations A3, A4, η, *S*, β, *T* refer to the phases Al_3Fe, Al_4Ca, $MgZn_2$, Al_2CuMg, $Al_2Mg_3Zn_3$, respectively

Table 3
Calculated critical temperatures of phase transformations in the investigated alloys

Phase	Temperature, °C			
	1Ca0Cu	1.5Ca0Cu	1.5Ca0.5Cu	1.5Ca1Cu
(Al)	619.3	613.2	617.0	615.6
Al_3Fe	598.8	583.5	583.4	584.6
Al_4Ca	548.7	563.9	567.2	565.8
T	459.7	458.2	480.3	483.3
T_S[1]	522.4	515.2	508.6	489.3
T_{NS}[2]	392.8	383.8	445.0	448.7
ΔT_{SSHT}[3]	62.7	57.0	28.3	6.0
ΔT[4]	96.9	98.0	108.4	126.3
ΔT_{DSC}[5]	87.9	83.3	90.1	88.7

[1]Equilibrium solidus temperature
[2]Non-equilibrium solidus temperature
[3]The range of processing temperatures at which a solid solution is obtained
[4]Equilibrium interval of crystallisation
[5]Crystallisation interval according to DSC data **(Fig. 2)**

subsequently $Al_2Mg_3Zn_3$. It is evident from the data presented in **Table 3** that the liquidus temperatures of the alloys are closely spaced. Conversely, the equilibrium solidus temperatures of the alloys with copper, as determined by calculations, were found to be lower. However, the temperatures of the crystallization onset of phase *T* were observed to be higher. Consequently, the processing interval for these alloys to achieve a solid solution is found to be constrained, particularly for the 1.5Ca1Cu composition. This complicates the heat and deformation treatment regime in the long term.

The polythermal cross-section on the calcium side, when considered in isolation and without regard for the influence of copper **(Fig. 1, *e*)**, demonstrates that an augmentation in the calcium fraction results in a reduction in the liquidus temperature and a constriction of the treatment interval for solid solution obtaining. The polythermal cross-sections at constant magnesium (5.5%) and calcium (1% and 1.5%) contents are almost indistinguishable (see **Fig. 1, *f***, which shows the calculation for the 1.5Ca0Cu alloy). According to this, alloys containing up to 2% zinc in the solid state at room temperature should contain two non-equilibrium phases: Al_3Mg_2 (β) and $Al_2Mg_3Zn_3$; and only the $Al_2Mg_3Zn_3$ phase for more than 2%. In view of the high solubility of zinc in Al_4Ca, it is imperative to ensure zinc levels remain at least 3%. As illustrated in **Fig. 1, *g***, the polythermal cross section on the copper side is depicted at constant average concentrations of magnesium (5%), calcium (1.65%), and zinc (3.74%). This demonstrates that the region of existence of supersaturated solid solution is slightly wider compared to the values given in **Table 2**. It is anticipated that with an increase in copper content beyond 2%, the presence of the copper-containing *S*-Al_2CuMg phase will become evident within the cast structure.

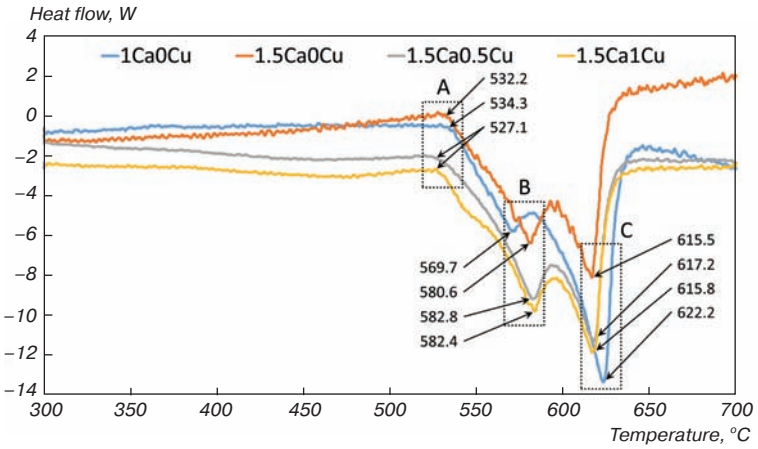

Fig. 2. Heating curves of the investigated alloys

Study of phase composition after casting and heat treatment

As illustrated in **Fig. 2**, the DSC heating curves demonstrate three distinct regions in the cast state: an inflection point (area *A*), and endothermic peaks (areas *B* and *C*). The inflection points refer to the solidus temperatures. It is evident from the data presented in **Table 3** that the discrepancy between the experimental and calculated equilibrium solidus temperatures for alloys devoid of copper is minimal. However, for alloys containing copper, these temperatures are significantly higher than the calculated values **(Table 3)**. The B peak is indicative of the dissolution of the Al_4Ca phase, also known as $(Al,Zn)_4Ca$. It is evident that with an increase in calcium content, there is a concomitant increase in the intensity of the peak. Peak C is attributed to the dissolution of (Al), and alloys containing 1.5% Ca demonstrate negligible differences in this parameter. It seems that due to the small fraction of non-equilibrium phases, their dissolution could not be detected in the temperature range from 450 to 500 °C. The calculated crystallization interval for all alloys was found to be less than 100 °C. This finding indicates a comparable level of casting properties to the alloy AMg10 [23].

Fig. 3 presents images of microstructures in the cast state. It is evident that the alloys do not exhibit submicron eutectic structures, a property that is commonly observed in alloys containing calcium [8]. Instead, the eutectic exhibits a degenerate character. With an increase in calcium content, the eutectic crystal shape transitions from an elongated (1Ca0Cu) to a partially fragmented (other alloys) morphology. The statistics of the size distribution of the second phases are presented in the insets of the corresponding microstructure images. The distribution of particles differs significantly from that of normal crystals, with eutectic crystals exhibiting smaller sizes (up to 4 μm on average), but also elongated particles reaching up to 19 μm. Furthermore, calculations demonstrated an increase in size with rising calcium fraction

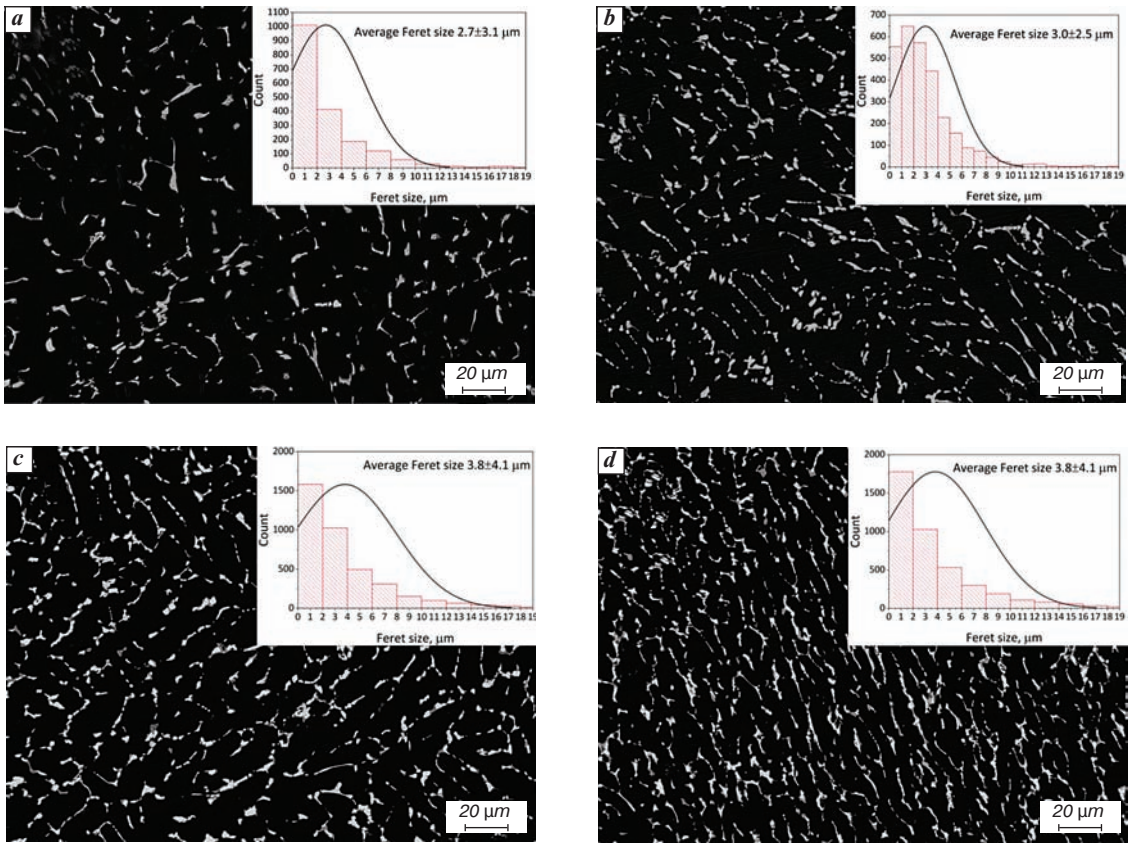

Fig. 3. SEM microstructures of the investigated alloys in the cast state, combined with the Feret particle size distribution of the secondary phases: *a* – 1Ca0Cu; *b* – 1.5Ca0Cu; *c* – 1.5Ca0.5Cu; *d* – 1.5Ca1Cu

and following copper addition. The volume fraction of secondary phases, as determined by Thermo-Calc data and ImageJ software is presented in **Table 4**. Preliminary calculations indicate that magnesium, zinc and copper participate in the formation of phase *T*, which is why its volume fraction is the largest among the secondary phases. When the calculated data on the volume fractions of Al_3Fe and Al_4Ca are taken into account, as well as the low diffusive mobility of calcium and iron in aluminium and the stability of the phases formed by them, it can be calculated that the real fraction of the *T* phase was between 1.5 vol.% and 4.5 vol.%. It is evident that the addition of copper increases the proportion of secondary phases.

Table 4
Calculated phase fractions in the investigated alloys

Phase	Q_V[1] (Q_M[2]) in alloy			
	1Ca0Cu	1.5Ca0Cu	1.5Ca0.5Cu	1.5Ca1Cu
Calculated in Thermo-Calc at 25°C[3]				
(Al)	77.74 (78.55)	73.86 (75.25)	75.70 (76.51)	77.63 (77.86)
Al_3Fe	0.53 (0.74)	0.33 (0.47)	0.32 (0.44)	0.36 (0.49)
Al_4Ca	3.72 (3.14)	7.34 (6.24)	7.14 (6.01)	6.92 (5.79)
T#1	18.01 (17.58)	18.46 (18.05)	16.14 (16.30)	15.09 (15.85)
T#2	–	–	0.71 (0.73)	–
Calculated in ImageJ (cast state)				
$Al_3Fe + Al_4Ca + T\#1 + T\#2$	5.54 ± 0.43	9.05 ± 0.45	10.65 ± 0.39	11.97 ± 0.57
Calculated in ImageJ (quench state)				
$Al_3Fe + Al_4Ca + T\#1 + T\#2$	4.99 ± 0.41	9.69 ± 0.91	8.03 ± 0.70	8.92 ± 0.71

[1]Volume fraction
[2]Mass fraction
[3]For the 1.5Ca1Cu alloy, the composition is given at 50°C due to the difficulty of constructing phase boundaries at lower temperatures.

The 1Ca0Cu alloy is characterised by the most contrasting phase composition (**Fig. 4, *a***). The presence of three distinct phases is evident in their colour and morphology: light and grey fragments, along with rare light needle-shaped crystals. Energy dispersive analysis showed that these phases are $(Al,Zn)_4Ca$, $Al_2Mg_3Zn_3$ and Al_3Fe (82.3 at.% Al; 9.7 at.% Mg; 0.7 at.% Ca; 1.9 at.% Zn; 5.4 at.% Fe), respectively. The composition of $(Al,Zn)_4Ca$, $Al_2Mg_3Zn_3$ phases is presented in the graphs in **Fig. 5**. With increasing calcium content (**Fig. 4, *b***) and copper addition (**Fig. 4, *c*, *d***), it becomes challenging to visually detect the presence of phases other than $(Al,Zn)_4Ca$. In alloys containing 1.5% Ca, the phases with iron exhibit a compact form.

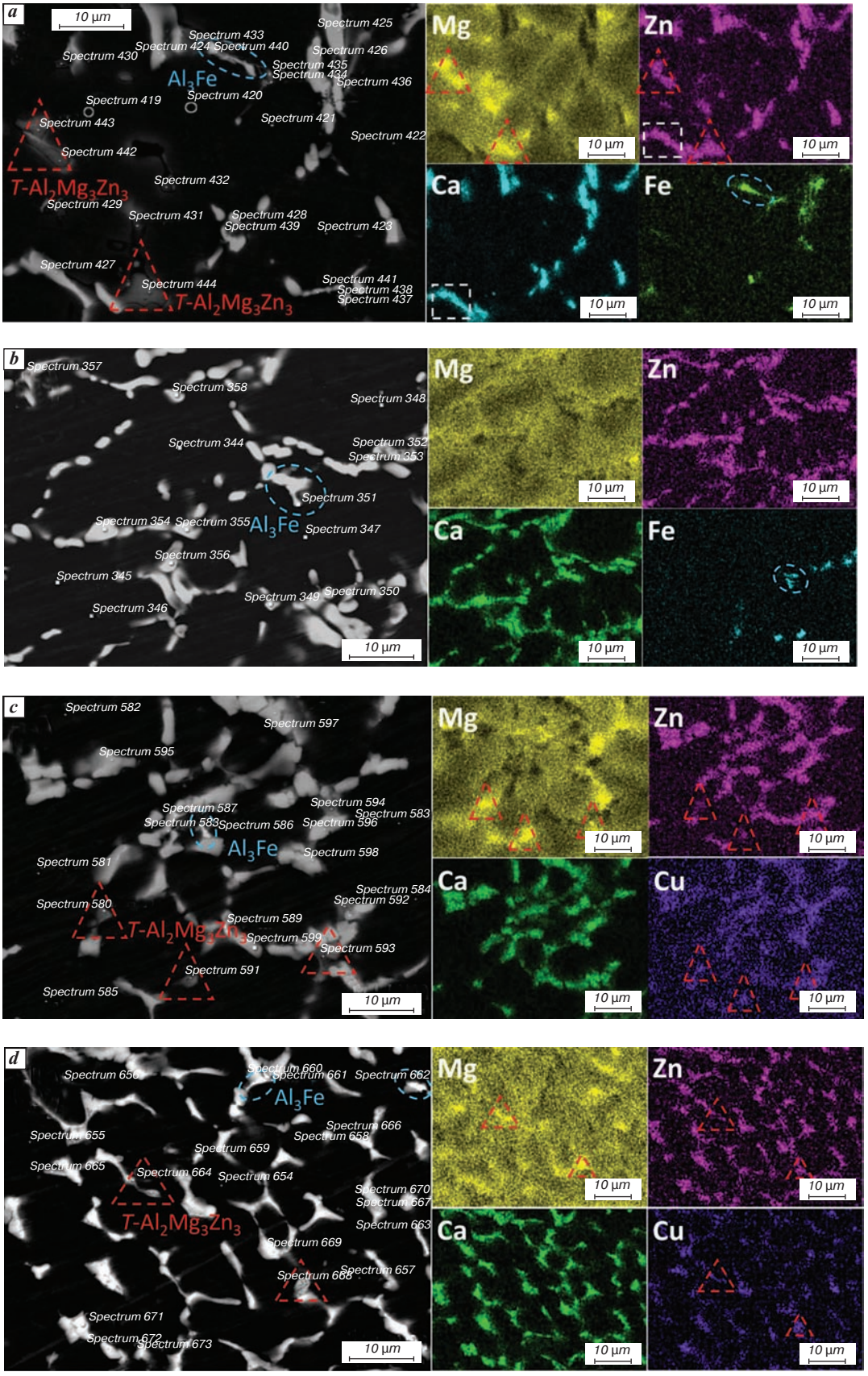

Fig. 4. SEM microstructures and corresponding element distribution maps of the investigated alloys in the cast state: *a* – 1Ca0Cu; *b* – 1.5Ca0Cu; *c* – 1.5Ca0.5Cu; *d* – 1.5Ca1Cu

As illustrated in the graphs in **Fig. 5, *a*** (solid lines), there is a change in the solid solution composition as a function of the alloy composition in the cast state. It is noteworthy that the Zn content in (Al) remains practically unchanged in all alloys. Concurrently, the Cu content in (Al) rises in proportion to its concentration, though remains at a low level. More noticeable changes can be seen in the graphs showing the dependence of the composition of the Al_4Ca phase on the alloy composition (**Fig. 5, *b***, solid lines). It is evident that zinc solubility diminishes in proportion to increasing calcium and subsequently copper content within the alloy. Conversely, the solubility of copper increases with its increasing content in the alloy. The change in the composition of the *T* phase is shown in **Fig. 5, *c*** (solid lines). It is evident that the maximum magnesium content in the phase is observed in alloy 1.5Ca0Cu. Following this, a decrease in magnesium concentration is evident due to the addition of copper. It is notable that the zinc content remains constant at 1.5% Ca, which is 2 times lower than that at 1% Ca.

As demonstrated in **Fig. 1**, the calculations indicate that a temperature of 440 °C should be adequate to dissolve the *T*-phase in both the 1Ca0Cu and 1.5Ca0Cu alloys. The presence of copper has been shown to enhance the thermal stability of this phase, and its presence should be discernible in the other two alloys. Furthermore, the quenching process led to qualitative alterations in the structure at 1% Ca, manifesting as fragmentation and spheroidization of the $(Al,Zn)_4Ca$ phase crystals **(Fig. 6, *a*)**. In compositions other than those examined, no significant changes were revealed. As demonstrated in **Fig. 5, *a***, the magnesium content in (Al) increased by 1.5 times due to the dissolution of non-equilibrium phases. However, an increase in zinc content in the alloy was only observed in the alloy with 1% Ca. Conversely, at 1.5% Ca, a slight decrease was observed. This phenomenon can be attributed to the fact that, at 1% Ca, the volume fraction of the Al_4Ca phase is minimal, resulting in increased zinc dissolution into the *T* phase **(Fig. 5, *c*)**. However, this *T* phase subsequently disappears following quenching. Conversely, the graph in **Fig. 5, *b*** (dotted line) demonstrates an enhancement in zinc solubility in Al_4Ca following heat treatment, which accounts for the reduction in its proportion within (Al).

As anticipated, the temperature of 440 °C proved to be insufficient for complete dissolution of the *T* phase in alloys with copper. Consequently, grey intermetallides surrounding the $(Al,Zn)_4Ca$ phase can be observed in **Fig. 6, *c***. In the 1.5Ca1Cu alloy **(Fig. 6, *d*)**, only micron particles corresponding to phase *T* could be identified. The changes in the composition of this phase are reflected in the graph (**Fig. 5, *c***, dotted line). However, the interpretation of these changes is hindered by the limited size of the analysed objects.

In order to achieve a more precise characterisation of the phase composition of alloys, samples were obtained and investigated following cooling with the furnace **(Fig. 7)**. This method has been shown to promote the growth of phase sizes and facilitate a more complete diffusion flow, thereby enabling qualitative identification through the utilisation of SEM. As evidenced by the graphs in **Fig. 5, *a*** (dashed lines), the predominant trends in Mg/Zn/Cu content in (Al)/Al_4Ca are preserved. Concurrently, the phase composition of the 1Ca0Cu and 1.5Ca0Cu alloys mirrors that observed post-casting. However, differences appear in alloys containing copper. According to the calculation, there should be only one copper-containing phase in the solid state – *T*. The calculated concentration of copper in this phase is 13 wt.% (see **Table 2**). In the alloy after slow cooling, its concentration is slightly lower – 11 wt.%. In addition to the Al_3Fe, Al_4Ca and $Al_2Mg_3Zn_3$ phases, the presence of two additional copper-containing phases is evident. In the alloy 1.5Ca0.5Cu, the presence of light compact crystals consisting of aluminium (56.5 at.%), magnesium (27.2 at.%) and copper (10.8 at.%) is evident on the background of the *T* phase **(Fig. 7, *c*)**. The composition of these crystals does not correspond to any of the compounds that could be in equilibrium according to the calculated data for the Al – Mg – Zn – Cu system **(Fig. 1)**. According to [9], the most probable phase in alloys based on Al – Mg – Zn may be the AlCuMg phase, which can be in equilibrium with (Al) only in the presence of zinc. The observed discrepancy between the identified

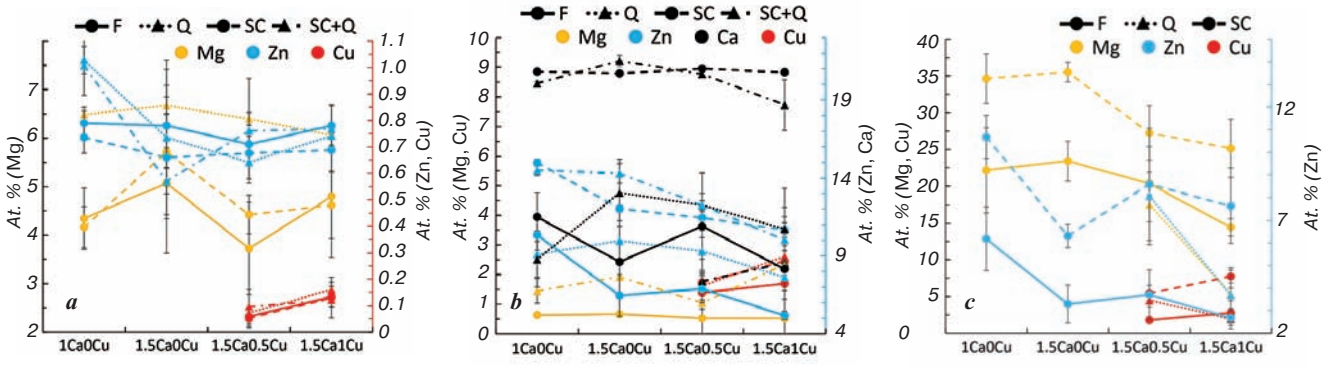

Fig. 5. Dependences of Mg, Zn, Ca and Cu content in phases:
a – (Al); *b* – Al_4Ca; *c* – *T*-$Al_2Mg_3Zn_3$. In the graphs, abbreviations *F*, *Q*, *SC*, *SC* + *Q* refer to the cast state, quenched state, furnace cooling and quenching after furnace cooling, respectively

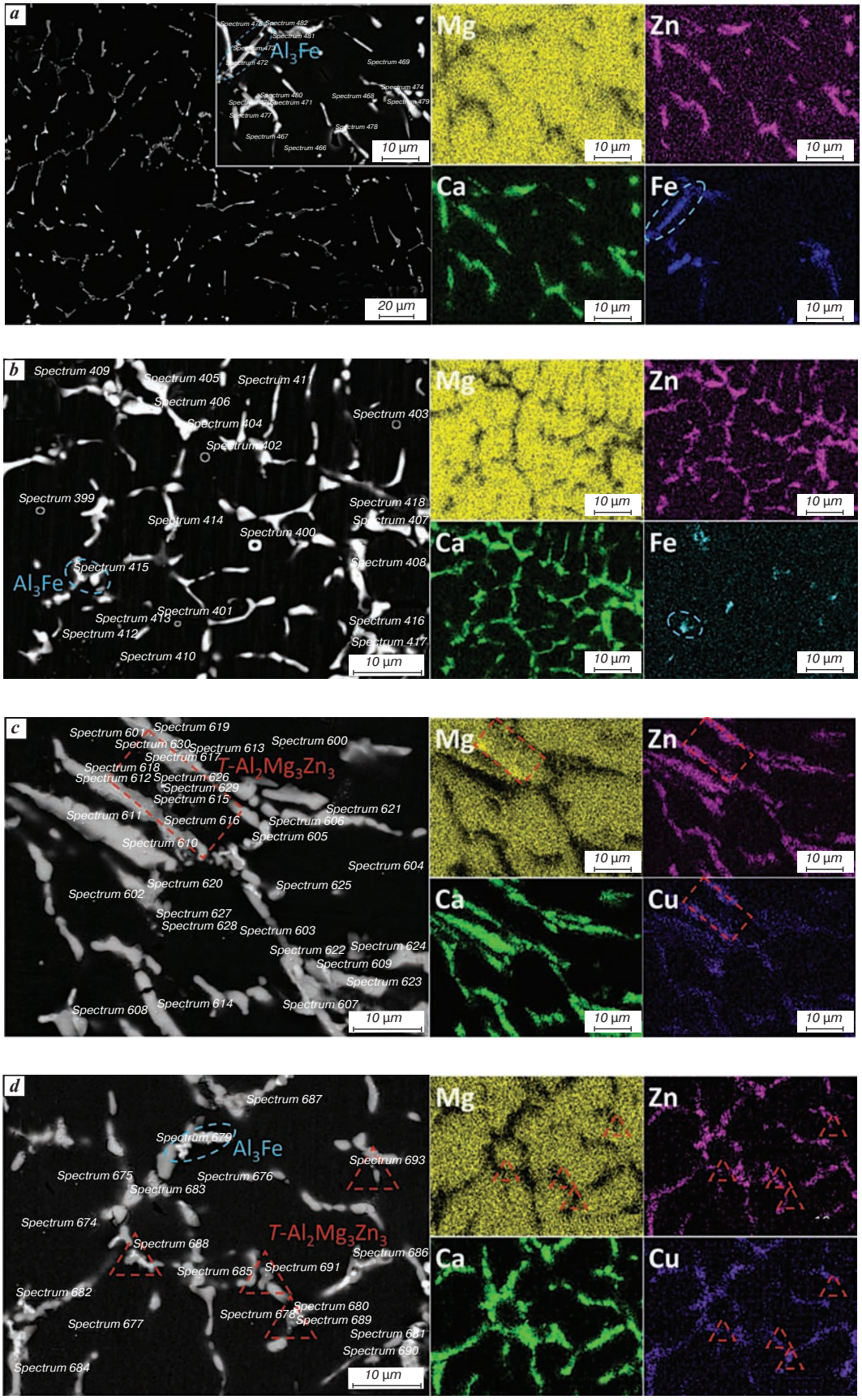

Fig. 6. SEM microstructures and their corresponding element distribution maps of the investigated alloys after quenching at 440 °C, 3 h: *a* – 1Ca0Cu; *b* – 1.5Ca0Cu; *c* – 1.5Ca0.5Cu; *d* – 1.5Ca1Cu

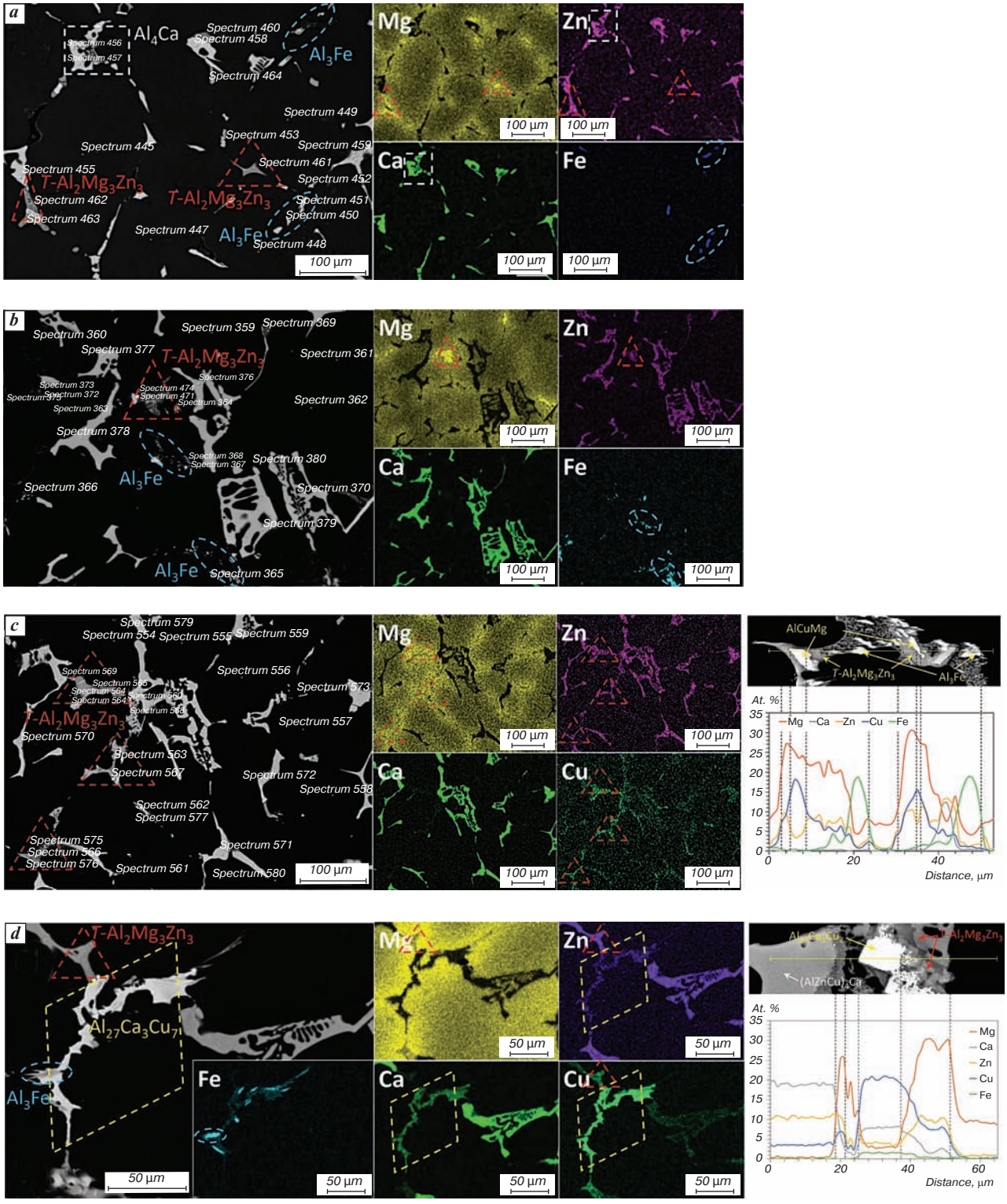

Fig. 7. Microstructures and their corresponding element distribution maps and line spectra of the investigated alloys after furnace cooling: *a* – 1Ca0Cu; *b* – 1.5Ca0Cu; *c* – 1.5Ca0.5Cu; *d* – 1.5Ca1Cu

compound's stoichiometry and the reference data can be attributed to its proximity to the *T* phase, where the 'illumination' of elements causes a distortion of the analysis results. With the increase of copper concentration up to 1.22%, the supposed AlCuMg phase is absent. Instead, the presence of large crystals of amorphous form or veins consisting of aluminium (64.8 at.%), calcium (8.4 at.%) and copper (18.4 at.%) is revealed, along with magnesium (2.8 at.%), iron (2.6 at.%) and zinc (6.1 at.%). In consideration of the extant literature pertaining to the Al – Ca – Cu system, it can be posited that the observed phase is designated as $Al_{27}Ca_3Cu_7$. The presence of this phase in the alloy does not contradict the assumed distribution of phase regions in the solid state [16]. The presence of this phase is consistent with the observed smaller proportion of zinc in the $(Al,Zn)_4Ca$ phase in the 1.5Ca0.5Cu alloy, given its distribution between the three phases: $(Al,Zn)_4Ca$, *T* and $Al_{27}Ca_3Cu_7$. No compound with the assumed formula $Al_2(Mg,Ca)$ has been identified in the course of studies [17–19].

In addition, the alloy samples were subjected to quenching following cooling with the furnace, a process analogous to that employed for the samples after casting. The solid solution composition (**Fig. 5, *a***, dashed-dotted lines) was found to be similar in magnesium and copper content to that after casting and quenching (dotted lines in **Fig. 5, *a***). However, significant discrepancies were observed in the zinc content of (Al). The nature of the changes in the copper-free alloys is analogous to that for the quenched state following casting. Concurrently, in copper-containing alloys, its content was equivalent to the cast state, though higher in comparison with the values directly subsequent to cooling with the furnace. In the Al_4Ca phase of the copper-containing alloys, the zinc fraction remained virtually unaltered (**Fig. 5, *b***, dashed-dotted lines), and the general character of the curve is analogous to the quench condition after casting (**Fig. 5, *b***, dotted lines). However, given the results obtained by SEM, it cannot be unequivocally stated whether zinc solubility in the Al_4Ca phase is enhanced, and a broader study to investigate this aspect is necessary.

Conclusion

1. The present study has utilised both computational and experimental methods of analysis to comprehensively investigate the phase composition of alloys within the Al – Mg – Zn – Ca – Cu system. The calculated data on the temperatures of the beginning and end of crystallization exhibited high convergence with practical results.

2. It was determined that the zinc content in the solid solution in the cast state is independent of the calcium and copper content in the alloy within the investigated compositions, and is at the level of 2 wt.%. (0.8 at.%). It is noted that zinc solubility in the Al_4Ca phase decreases with increasing calcium content.

3. The investigation of the phase composition subsequent to quenching at 440 °C for 3 h demonstrated that an enhancement in the solubility of zinc in (Al) is exclusively observed in the presence of 1% Ca, attributable to the dissolution of the non-equilibrium phase *T*. In the other alloys, the values of this parameter remained at the level of the cast state. The primary cause of this phenomenon was identified as the enhancement of zinc solubility within the Al_4Ca phase in alloys containing 1.5% Ca. An enhancement of zinc solubility in (Al) up to 2.5 wt.% was attained. In other alloys, an increase in zinc content within the Al_4Ca phase was observed subsequent to quenching, which was identified as the primary cause.

4. In the samples obtained by cooling with the furnace, it was revealed that the addition of 0.5% Cu leads to the formation of an additional copper-bearing phase, the composition of which corresponds to the compound S-Al_2CuMg. These crystals exhibit compact dimensions and are concentrated in proximity to the T-$Al_2Mg_3Zn_3$ phase. Furthermore, an increase in the copper content to 1% results in the formation of a ternary compound corresponding to the $Al_{27}Ca_3Cu_7$ phase, superseding the *S* phase. In addition to calcium and copper, magnesium, zinc and iron have been identified in the compound.

The study was carried out using the funds of the Russian Science Foundation grant No. 23-79-01055 (scanning microscopy, differential scanning calorimetry) and the funds of the P.L. Kapitsa grant of the Moscow Polytechnic University, implemented within the Priority 2030 programme (melting and casting, heat treatment). The structure study was carried out using the scientific equipment of the CKP NRC "Kurchatov Institute - IREA".

References

1. Gupta Sh., Singh D., Yadav A., Shambhav J., Bhanu P. A Comparative Study of 5083 Aluminium Alloy and 316L Stainless Steel for Shipbuilding Material. *Materials Today: Proceedings*. 2020. Vol. 28, Pt. 4. pp. 2358–2363.

2. Hosseinabadi O. F., Khedmati M. R. A Review on Ultimate Strength of Aluminium Structural Elements and Systems for Marine Applications. *Ocean Engineering*. 2021. Vol. 232, Iss. 10. 109153.

3. Zheng K., Politis D. J., Wang L., Lin J. A Review on Forming Techniques for Manufacturing Lightweight Complex—Shaped Aluminium Panel Components. *International Journal of Lightweight Materials and Manufacture*. 2018. Vol. 1. pp. 55–80.

4. Yun J., Kang S., Lee S., Bae D. Development of Heat-Treatable Al – 5Mg Alloy Sheets with the Addition of Zn. *Materials Science and Engineering: A*. 2019. Vol. 744. pp 21–27.

5. Carroll M. C., Gouma P. I., Mills M. J., Daehn G. S., Dunbar B. R. Effects of Zn Additions on the Grain Boundary Precipitation and Corrosion of Al-5083. *Scripta Materialia*. 2000. Vol. 42. pp. 335–340.

6. Meng Ch., Zhang D., Hua C., Zhuang L., Zhang J. Mechanical Properties, Intergranular Corrosion Behavior and Microstructure of Zn Modified Al – Mg Alloys. *Journal of Alloys and Compounds*. 2014. Vol. 617. pp. 925–932.

7. Nishi M., Matsuda K., Miura N., Watanabe K., Ikeno S., Yoshida T., Murakami S. Effect of the Zn/Mg Ratio on Microstructure and Mechanical Properties in Al – Zn – Mg Alloy. *Material Science Forum*. 2014. Vol. 794-796. pp. 479–482.

8. Belov N., Naumova E., Akopyan T. Eutectic Alloys Based on the Al–Zn–Mg–Ca System: Microstructure, Phase Composition and Hardening. *Materials Science and Technology*. 2017. Vol. 33, Iss. 6. pp. 656–666.

9. Mondolfo L. F. Aluminum Alloys: Structure and Properties. Butterworths: London-Boston, 1976. 982 p.

10. Belov N. A., Naumova E. A., Doroshenko V. V., Avxentieva N. N. Combined Effect of Calcium and Silicon on the Phase Composition and Structure of Al–10%Mg Alloy. *Russian Journal of Non-Ferrous Metals*. 2018. Vol. 59. pp. 67–75.

11. Karpova Zh. A., Shurkin P. K., Sivtsov K. I., Laptev I. N. Structure Formation and Processability of the Al –Zn – Mg –Ca –Fe –Zr –Sc Alloy at Hot Rolling and TIG Welding. *Izvestiya Vuzov. Tsvetnaya Metallurgiya*. 2021. Iss. 3. pp. 46–56.

12. Belov N., Naumova E., Akopyan T. Eutectic Alloys Based on the Al – Zn – Mg – Ca System: Microstructure, Phase Composition and Hardening. *Materials Science and Technology*. 2017. Vol. 33, Iss. 6. pp. 656–666.

13. Doroshenko V. V., Naumova E. A., Bazlova T. A., Samoshina M. E. Peculiarities of the Phase Composition and Microstructure of Al – Ca – Zn – Mg System Alloys. *Tsvetnye Metally*. 2017. No. 9. pp. 78–83.

14. Belov N. A., Naumova E. A., Akopyan T. K. Effect of Calcium on Structure, Phase Composition and Hardening of Al – Zn – Mg Alloys Containing up to 12wt.%Zn. *Materials Research*. 2015. Vol. 18, Iss. 6. pp. 1384–1391.

15. Letyagin N. V., Shurkin P. K., Nguen Z., Koshmin A. N. Effect of Thermodeformation Treatment on the Structure and Mechanical Properties of the Al3Ca1Cu1.5Mn Alloy. *Physics of Metals and Metallography*. 2021. Vol. 122. pp. 814–819.

16. Akopyan T. K., Belov N. A., Letyagin N. V., Cherkasov S. O., Nguen X. D. Description of the New Eutectic Al – Ca – Cu System in the Aluminum Corner. *Metals*. 2023. Vol. 13, Iss. 4. 802.

17. Doroshenko V., Shurkin P., Sviridova T., Fortuna A., Shkaley I. Phase Composition and Microstructure of Cast Al – 6%Mg – 2%Ca – 2%Zn Alloy with Fe and Si Additions. *Metals*. 2023. Vol. *13, Iss.* 9. 1584.

18. Doroshenko V. V., Korotkova N. O., Cherkasov S. O., Kalitina M. N. Composition and Stability of Al_2(Mg,Ca) Compound in Alloys of Al – Mg – Ca – (Zn) System. *Nonferrous Metals*. 2024. Vol. 1. pp. 49–56.

19. Doroshenko V. V., Aksenov A. A., Mansurov Yu. N. Effect of Iron Impurity on the Structure and Phase Composition of Al – 6% Mg – 2% Ca – 2% Zn alloy. *Tsvetnye Metally*. 2023. No. 6. pp. 73–83.

20. Pan Y., Zhang D., Liu H., Zhuang L., Zhang J. Precipitation Hardening and Intergranular Corrosion Behavior of Novel Al – Mg – Zn(-Cu) Alloys. *Journal of Alloys and Compounds*. 2021. Vol. 853. 157199.

21. Cao Ch., Zhang D., Wang X., Ma Q., Zhuang L., Zhang J. Effects of Cu Addition on the Precipitation Hardening Response and Intergranular Corrosion of Al – 5.2Mg – 2.0Zn (wt.%) Alloy. *Materials Characterization*. 2016. Vol. 122. pp. 177–182.

22. Thermo-Calc Software TTAL5 Al-Alloys. URL: www.thermocalc.com (Accessed Date: 20.03.2025).

23. Doroshenko V. V., Barykin M. A., Vasina M. A., Aksenov A. A. Combined Effect of Calcium and Zinc on the Hot Cracking of Al – Mg Alloys. *Tsvetnye Metally*. 2022. No. 12. pp. 45–54.

NFM